Published in final edited form as:
Surgery. 2011 May ; 149(5): 689–698. doi:10.1016/j.surg.2011.02.007.

Hands-free, Wireless Goggles for Near-infrared Fluorescence and Real-time Image-guided Surgery

Yang Liu[a,b], **Adam Q. Bauer**[a], **Walter Akers**[a], **Gail Sudlow**[a], **Kexian Liang**[a], **Duanwen Shen**[a], **Mikhail Berezin**[a], **Joseph P. Culver**[a,b], and **Samuel Achilefu**[a,b,*]

[a]Department of Radiology, Washington University, St. Louis, MO 63110, USA

[b]Department Biomedical Engineering, Washington University, St. Louis, MO 63110, USA

Abstract

Background—Current cancer management faces several challenges, including the occurrence of residual tumor after resection, the use of radioactive materials or high concentrations of blue dyes for sentinel lymph node (SLN) biopsy, and use of bulky systems in surgical suites for image guidance. To overcome these limitations, we developed a real-time intraoperative imaging device that, when combined with near infrared (NIR) fluorescent molecular probes, can aid identification of tumor margins, guide surgical resections, map SLNs, and transfer acquired data wirelessly for remote analysis.

Methods—We developed a new compact, wireless, wearable, and battery-operated device that allows hands-free operation by surgeons. A CCD-based consumer-grade night vision viewer was used to develop the detector portion of the device and the light source portion was developed from a compact headlamp. This piece was retrofitted to provide both NIR excitation and white light illumination simultaneously. Wireless communication was enabled by integrating a battery-operated miniature radio-frequency video transmitter into the system. We applied the device in several types of oncologic surgical procedures in murine models, including SLN mapping, fluorescence-guided tumor resection, and surgery under remote expert guidance.

Results—Unlike conventional imaging instruments, the device directly displays fluorescence information on its eyepiece. When employed in SLN mapping, the locations of SLNs were clearly visualized, even with tracer level dosing of a NIR fluorescent dye, indocyanine green. When utilized in tumor resection, tumor margins and small nodules not visible to the naked eye were readily visualized. In a simulated point-of-care setting, tumors were successfully located and removed under remote guidance using the wireless feature of the device. Importantly, the total cost of this prototype system ($1200) is significantly lower than existing imaging instruments.

Conclusion—Our results demonstrate the feasibility of using the new device to aid surgical resection of tumors, map SLNs, and facilitate telemedicine.

*Corresponding Author: Samuel Achilefu, Ph.D, Department of Radiology, Washington University School of Medicine, 4525 Scott Avenue, St. Louis, MO 63110, USA, Tel: 314-362-8599, achilefus@mir.wustl.edu.

Competing Interests Statement
The authors declare that they have no competing financial interests.

Introduction

Without image guidance, surgeons are required to remove large surgical margins around what they perceive as tumor due to the similarity of diseased to surrounding healthy tissues. In some parts of the body such as the brain, surgeons do not have the luxury of removing sizeable healthy tissue for fear of inducing irreparable damage to complex brain physiology. Despite progress made to enhance contrast between tumor and normal tissues, the human eye is not capable of detecting the contrast signals with high sensitivity in the operating room (OR). This limitation further exasperates adequate tumor resection, resulting in the presence of cancerous cells at or near the boundaries of surgically removed tissues[1, 2]. However, recent advances in medical imaging technologies have facilitated the use of imaging instruments to guide surgery in the OR. Besides unsatisfactory sensitivity and accuracy, modern intraoperative imaging modalities suffer from high cost, complex instrumentation and time-consuming image analysis, further limiting accessibility of *bona fide* standard of cancer care available to patients. For sentinel lymph node (SLN) biopsy, the standard breast cancer staging procedure can also cause adverse effects on patients and healthcare workers[3–7]. For instance, radioactive tracers emit hazardous ionizing radiation to patients as well as surgeons[4, 8] and the large doses of blue dyes used for visualizing SLNs with the naked eye may cause adverse reactions [3, 5–7]. Moreover, some surgical procedures often require a team of experienced oncologic surgeons, radiologists and pathologists to work together, who are oftentimes not available in most rural clinics and developing countries. To address these challenges, there is a compelling need for accurate, affordable, user-friendly, portable, and versatile intraoperative imaging system. Not only should they offer real-time imaging capability in a confined surgical suite, they should also be able to bring remote collaborative efforts from geographically separated medical professionals to the bedside.

The high detection sensitivity and use of non-ionizing radiation have facilitated the development of several optical systems to detect and assess tumor margins[9–18]. However, most of these systems require graphic display of results on a monitor, which can distract surgeons from focusing on critical surgical resection of tumors.

To overcome the above limitations, we have designed a goggle-based device that does not require remote monitoring. The system is affordable, battery-operated, compact, wireless, wearable, and allows hands-free surgical operation (Fig.1A). The overall design of system is illustrated in Fig. 1B. With this device, functional information provided by near infrared (NIR) fluorescence of molecular probes can be directly displayed with adjustable amplification on its goggle eyepiece. Both NIR light-emitting diode (LED) and NIR-depleted visible LEDs served as integrated light sources on the device, providing concurrent fluorescence excitation of NIR molecular probes and illumination of the surgical field. Consequently, the device is designed to allow one eye to capture the functional information from the NIR fluorescence while the other eye can view both tumor and surrounding tissue anatomy with unaided eyepiece. The system is further equipped with the capability to transfer wirelessly real-time video to a remote site, where the current view for the goggle wearer can be graphically displayed. An expert at the remote site can see what is happening during the surgery from the point of view of the local surgeon and provide expert advice and comprehensive image analysis if needed. Hence, the new system can be potentially applied to point-of-care medical interventions, real-time pathological assessment of tissues, and remote medical consulting.

Materials and Methods

Imaging Device

The detector portion of the device consists of an off-the-shelf night vision viewer (iGEN NV20/20-IC, First Texas Products, El paso, TX, USA) that utilizes a Sony ICX254AL diagonal 6mm CCD image sensor. Default objective lens of iGEN NV20/20-IC was employed. An emission filter was mounted on the objective lens. The 830nm band pass filter (#302470, CVI Melles Griot, Albuquerque, NM, USA) was selected for SLN mapping application, whereas the 820nm long pass filter (#8480, Omega Optical, Brattleboro, VT, USA) was used for tumor imaging. The light source portion of the system is a modified headlamp (Trailfinder Series 6 LED Headlight, Energizer, St. Louis, MO, USA). This headlamp was converted to a light source by disconnecting two central white LEDs and replacing them with two 770nm NIR LEDs (#LED770-03AU, total radiated power of 18mW at 50mA, Roithner Lasertechnik, Vienna, Austria). Two additional peripheral white LEDs were left intact to provide white light illumination. The NIR light is collimated by existing optics, which provides a field of view approximately 0.3m in diameter at 1 m. All LEDs are driven by an onboard circuit powered by three AAA batteries. No excitation filter was used for SLN mapping but a 775nm short pass filter (#NT64–615, Edmund Optics, Barrington, NJ, USA) was mounted onto to the headlamp for tumor imaging. The detector and light source were mechanically integrated onto a customized helmet allowing hands free operation of the device For real-time video transfer during operation, the device was connected to a RCA composite cable, and then to a USB video capture cable (#SVID2USB2NS, Startech, Lockbourne, OH, USA) that was plugged into a laptop computer (T500, Lenovo, Morrisville, NC, USA). For wireless video transfer, a pocketsize RF transmitter/receiver set (#SCI-PVTS2, Spy Chest, Crestview, FL, USA) replaced the RCA composite cable for completely connection-free use. For all studies, the device was set to operate at a video rate of 12 frames per second (fps) and a working distance of 0.5m. Fluorescence images were acquired with the device's NIR sources, while white light images were acquired under room light illumination. All images and videos were acquired and stored using frame grabbing software (GrabBee). For detection sensitivity measurements, three parallel samples (n=3) of indocyanine green (Sigma-Adrich, St. Louis, MO, USA) in DMSO at various concentrations (0nM, 1nM, 3nM, 5nM, 7nM and 9nM) were prepared in a 96-well assay plate (#3603, Corning Incorporated, Corning, NY, USA) and imaged. Mean intensity values for individual wells were measured by ROI analysis in ImageJ and subsequently evaluated by linear regression against the known concentrations.

NIR Contrast Agents

Indocyanine green was purchased from Sigma-Adrich (St. Louis, MO, USA). MMPSense FAST 750 was purchased from VisEn (Waltham, MA, USA). LS301 was synthesized by literature method19, except that CEM microwave peptide synthesizer and Gilson HPLC system were used to prepare the peptide and purify the final product. The molecular probe consists of cysteine-glycine-arginine-aspartic acid-serine-proline-cystein-lysine peptide sequence and a near infrared fluorescent dye, cypate. This dye has absorption and emission maxima around 780nm and 830 nm, respectively, in biological media. The dye-peptide conjugate (LS301) was characterized by spectroscopic methods, analytical HPLC, and electrospray ionization mass spectrometry.

Animal Models

All animal procedures were conducted in compliance with Washington University Animal Studies Committee’s requirements for the care and use of animals in research. Six-week-old male C57B mice and male NCR nude mice were purchased from Taconic Farms (Hudson, NY, USA). For animal studies, the mice were anesthetized with ketamine and xylazine

cocktail (80 mg/kg and 13 mg/kg, respectively, intraperitoneal injection). The hair overlaying the region of interest was removed by gentle clipping and cream depilatory (Sally Hansen, Morris Plains, NJ, USA). The mice were killed immediately after imaging experiments by IP injection of 150 mg/kg sodium pentobarbital (Somnosal, MedVet, Worthington, OH, USA).

Sentinel Lymph Node Mapping

For SLN mapping, 6-week old male C57 black mice (Taconic Farms, Hudson, NY, USA) (n=5) were anesthetized and 3.75nmoles of indocyanine green in PBS solution were administered intradermally into both front paws (n=5×2). The subcutaneous axillary region was exposed by incising and retracting the overlaying skin. NIR and white light on the imaging device were simultaneously turned on, providing both fluorescence excitation and surgical field illumination. SLNs were identified and resected under image guidance. After resection, surgical sites were inspected thoroughly with the device under different signal amplification settings. For comparison, ischiatic lymph nodes were also excised and imaged as non-fluorescent controls. SLNs and control lymph nodes were examined with the system *ex vivo*. Excised tissues were embedded in Tissue-Tek OCT medium (Sakura Finetek, Torrance, CA, USA) and stored at −80 °C.

Fluorescence-guided Tumor Resection

For tumor imaging, 200,000 4T1*luc* cells were injected subcutaneously in both sides of the chest (n=5×2) of 6-week old male nude mice. Approximately 2 weeks after cell injection, mice were anesthetized with ketamine and xylazine as described above. LS 301 solution (100 μL of 100μM in 20% DMSO/80% saline) was injected intravenously via lateral tail vein. At 24 hours post-injection, non-invasive bioluminescence images and digital radiographs of the mice were acquired with the In-Vivo Multispectral FX PRO (Carestream Health, Inc. Rochester, NY). For bioluminescence imaging, luciferin (150 mg/kg) was injected intraperitoneally 5 minutes prior to imaging. Luciferin is a substrate for the enzyme luciferase needed to generate bioluminescence, which was detected by 5-minute exposure with 8×8 binning. Digital radiographs were acquired by 90-second exposure using the radiographic phosphor screen. Fluorescence-guided surgeries were subsequently carried out using the new goggle device. A midline incision was made from sternum to throat and skin reflected laterally to expose the mammary tissues. Tumor tissues were identified and resected under image guidance. In three cases, partial resections around the tumor margins were performed to demonstrate the capability of identifying residual tumor tissues. Surgical sites were then re-examined, to find residual cancerous tissues and small tumor nodules. Resected tumor and muscle tissues were examined *ex vivo* to compare fluorescence in tumor to non-tumor tissue. Tissues were subsequently embedded with Tissue-Tek OCT (Sakura Finetek, Torrance, CA, USA)and frozen for histology.

Tumor Resection under Telemedical Advising

Nude mice with 4T1*luc* tumor implanted subcutaneously in the right flank were anesthetized. MMPSense 750 FAST solution (100 μL of 20 μM in PBS) was injected intravenously via lateral tail vein. At 24 hours post-injection, fluorescence-guided tumor resection was performed in a simulated point-of-care setting using the new imaging system. Overlying skin was incised and reflected to expose the subcutaneous tissues. Fluorescence of the cancerous tissues was detected with the device. Real-time florescence videos were transferred wirelessly to a remote computer during surgery using the RF transmitter/receiver set described above. Surgical instructions by a remote scientist were relayed back to the lab via a mobile phone.

Histology and Microscopy

Resected lymph nodes, tumors, and control tissues were frozen in OCT. The tissues were sectioned in the cryostat to 8 microns thickness. For fluorescence microscopy, slides were taken directly from the −80 °C freezer to the Olympus BX51 upright epifluorescence microscope (Olympus America, Center Valley, PA, USA). Images were acquired for NIR (775+/−50 nm excitation, 810 nm longpass dichroic, and 845+/−55 nm emission filters) and Green (480+/−40 nm excitation, 505 nm longpass, and 535 emission filters) fluorescence as well as brightfield. NIR fluorescence, green autofluorescence and brightfield images were merged together to create composite images in ImageJ. The same slides were then stained with hematoxylin and eosin (H&E). Matching regions with fluorescence microscopy were found and imaged.

Results

Sentinel Lymph Node Mapping

Our prototype device is currently designed to work with NIR fluorescent probes with excitation and emission wavelengths centered at 780 nm and 830nm, respectively. Representative examples of NIR fluorescent dyes include indocyanine green, an FDA-approved NIR dye20, 21, and cypate, a readily functionalized indocyanine green analog 22. We demonstrate that the device can detect fluorescence from as low as 1 nM of indocyanine green dye (Fig. 1C).

We applied the prototype device in two types of oncologic surgical procedures to demonstrate the potential of the system in fluorescence-guided surgery. First, device was applied in SLN mapping in a murine model. We administered 3.75nmoles of indocyanine green solution intrademally into both forepaws of five mice (n=10). Indocyanine green subsequently migrated into surrounding lymphatic vessels and accumulated in the lymph nodes on both sides within 5 minutes post injection. SLNs were clearly tracked (Fig. 2A–C, Movie 1 [online]) and subsequently excised under real-time guidance of our device (Fig. 2D). After excision, surgical sites were thoroughly re-examined with the device under multiple signal amplification ranges. The SLNs were further confirmed by histological findings (Fig. 2E).

Fluorescence-guided Tumor Resection

Having demonstrated the feasibility of imaging SLNs, we further explored the potential of using the new device for guiding tumor resection and detecting non-obvious small tumor nodules. For this study, we used a NIR fluorescent molecular probe, LS 301. LS 301 is an imaging agent developed in our lab that preferentially binds to tumor margins (Fig. 3A). It is composed of a peptide sequence that binds integrin receptors on proliferating tumors and a near infrared fluorescent dye that is used for optical imaging, with a fluorescence peak centered at 830 nm. These features make LS 301 attractive for use in assessing surgical margins intraoperatively, which is suitable for our goggle study.

4T1-luc orthotopic mammary tumor model was used for this study. Although ectopic tumor models are widely used in cancer research, orthotopic tumor models generally present a more realistic natural state of the cancer, as tumors may behave differently in different tissues. Five mice that bore 4T1-luc mammary tumors in both breasts were studied (n=10). Briefly, 10 nmol of LS 301 solution was injected intravenously via lateral tail vein. At 24 hours post-injection, fluorescence-guided surgical removal of the tumors were carried out with the aid of the imaging device. Bioluminescence imaging was conducted to confirm the presence and position of cancer prior to surgery (Fig. 3B). High fluorescence signal at the tumor regions were observed when imaging non-invasively (Fig. 4A). The fluorescence

contrast between tumors and normal tissues was high, despite attenuation by scattering and absorption of light in the skin and overlying tissue. Tumors were subsequently resected under guidance of imaging device. The system was able to clearly delineate tumor margins (Fig. 4B, Movie 2 [online]). With direct visualization of tumor margins, surgical margins could be improved by minimizing the amount of surrounding healthy tissues removed. Residual tumors and small nodules that are not obvious to the naked eye were detected with the goggle system (Fig. 4B). LS 301 rapidly distributes throughout the body immediately after intravenous injection. Preferential uptake in the tumor and rapid clearance from non-target tissues within 1 hour post injection leads to high contrast in the target tissue. After surgery, organs were examined *ex vivo* at 24 hours (Fig. 4C). Biodistribution studies show that LS 301 is excreted through hepatobiliary and renal pathways. Consequently, in addition to the high tumor uptake that persists up to 24 hours post injection of the imaging agent, significant amounts of the probe is retained in the liver and kidneys, which correlates with the probe's excretion pathway. Histological assessments confirmed the malignant nature of the excised tissues and microscopy further revealed high fluorescence level in the tumor margins (Fig. 4D).

Tumor Resection under Telemedical Guidance

A unique advantage for telemedicine provided by this system is the ability to relay the actual point-of-view of the goggle wearer to a remote expert. In contrast, a static system would not capture the change in gaze direction as the local surgeon rotates his or her head up/down or left/ right. To test initial feasibility of this concept, we evaluated the new system with wireless data transfer in a telemedicine simulation. We limited the scope of this study to traditional radio-frequency (RF) communication, where the prototype device was coupled to a pocketsize RF transmitter/receiver set. Our device is also capable of coupling with other wireless communication methods such as 3-G networks. Using the RF transmitter, we conducted a fluorescence-guided tumor resection procedure in a simulated remote point-of-care setting. In this experiment, we used a commercial fluorescent molecular probe (MMPSense 750 FAST) to explore the capacity of our device to detect fluorescence signals from diverse optical imaging probes that operate through different contrast reporting strategies. Unlike LS 301 that preferentially binds to protein receptors on margins, the fluorescence from MMPSense 750 FAST is only detected in tumors with high expression of active matrix metalloproteinases (MMPs). High levels of MMP expression is a biomarker of highly proliferating tumors. MMP-mediated contrast mechanism offers lower background and higher signal to noise ratio compared to conventional fluorescent probes. By accessing the MMP activity in tumors, progression of cancer and therapeutic effects of anti-cancer treatments may be monitored24. In this situation, an experienced oncologist could guide the assessment of tumors from remote sites. . In this study, the functional status of the tumor was imaged by a veterinarian performing the surgery through the eyepiece and simultaneously transferred wirelessly to the computer of a remote imaging scientist (Fig. 5). The video was displayed in real time, enabling remote assistance. Based on the data transmitted, the scientist interacted verbally in real-time with the veterinary surgeon in the lab through a mobile phone to guide the surgery. Tumors were successfully located and removed under the wireless collaboration and the functional information of tumor status (MMPs activity) was stored at a remote computer. While this simulation simplifies clinical conditions, it illustrates the potential this imaging device holds for telemedicine and point-of-care applications.

Discussion

Incomplete tumor resection is a major factor that compromise long-term survival rate of cancer patients. Fluorescence-guided surgery is an emerging technology that holds great

potential to provide a viable solution to this problem. In this study, we developed and demonstrated the use of a new device that can detect non-obvious small tumor lesions, guide SLN biopsy and allow remote telemedical guidance.

To date, most fluorescence-guided intraoperative imaging modalities are limited to 2-D planar imaging due to the technical difficulties in implementing tomography in real time. In reality, 2-D imaging systems do not provide sufficient depth-information to guide surgery that is 3-D in essence. Although a 2-D functional-anatomical composite image could be projected on a monitor10, 25, surgeons still use naked eyes to survey the actual tissue anatomical landscape in real time. To overcome this obstacle, our system is designed as a goggle device that does not require remote display on a computer monitor. During operation, surgeons can simultaneously view the functional status in the eyepiece with one eye and obtain the anatomical information to navigate the region of interest with the unaided eye.

Without cost-effectiveness, any image-guided technology could not be readily translated into clinics on a global scale, regardless of its efficacy. Hence, an important component of our design process was to reduce the instrument cost and size, with the long-term goal of extending its use to underserved populations and rural areas. For instance, instead of building a detector from high-end scientific grade cameras that are generally large and expensive such as FLARE10 and Hamamatsu Photodynamic Eye26, the detector portion of the device was developed from a CCD-based consumer-grade night vision viewer. We have demonstrated the detector is able to provide high detection sensitivity *in vivo* along with low cost and compact size.

The detector operates on four AA batteries and offers 10 levels of adjustable gain settings. Each gain setting corresponds to a dynamic range of signal amplification that automatically optimizes and displays the detected NIR light level. This dynamic amplification feature is crucial for surgical applications, as it automatically optimizes and normalizes the fluorescence intensity displayed in real time. This circumvents the need to tediously re-adjust settings manually with specialized image-processing software in the dynamically changing surgical environment. In addition, the simple gain-setting control on the device allows the surgeon to manage the device directly, without the assistance of other personnel. These features could significantly simplify the procedures and lower the labor cost in the OR.

We demonstrated that the prototype device provides high detection sensitivity and signal-to-background contrast, which can help surgeons to locate non-obvious small cancerous lesions and SLNs. When utilized in tumor resection, the device detected tumor margins, small nodules, and some residual tumors that are not detectable with the unaided eye. This approach may improve surgical margins by reduce the size of healthy tissues resected, minimize the probability of incomplete resection, and decrease the need for follow-up surgery. When employed in SLN mapping, the device can clearly indicate the positions of SLNs even with tracer level dosing of indocyanine green, which circumvents the potential side effects caused by radioactive tracers and blue dyes.

In this study, wireless communication is enabled by integrating a battery-operated miniature RF video transmitter into the system to test initial feasibility of this concept. Coupling our device to standard communication platforms such as 3-G will facilitate real-time visual/auditory collaborative relations, as demonstrated in this study. Thus, direct communication can be made between clinicians at leading medical institutions and their counterparts in rural or remote areas, even across continents. The total cost of the prototype system is approximately $1,200, up to 100 times less than previously reported intraoperative fluorescence imaging systems such as FLARE™ (approximately $120,000)10, Hamamatsu

Photodynamic Eye (approximately $40,000)26 and GE FIGS system (approximately $15,000)25.

There are limitations to the study. Murine models were used to demonstrate the feasibility of image-guided SLN biopsy and tumor resection with our device. However, large animal models are needed to simulate human studies, which is the subject of a second-generation device. Additionally, the monocular visualization system may affect depth perception and require surgeons to use their dominant eyes for the goggle piece. This may present some logistical problems for the surgeon. Finally, our first prototype is not the optimal ergonomic design for any surgeon. In this prototype, we aim to demonstrate the concept rather than translating it into clinics in its current form. The next generation device will be smaller, lighter, with more functionalities and better ergonomics.

In summary, we have demonstrated the development and feasibility of using a hands-free and wireless device for NIR fluorescence-guided surgery. The device facilitated tumor resection and SLNs biopsy procedures. Furthermore, the device is affordable, portable, user-friendly, and provides the surgeon with wireless communication in a telemedicine setting, facilitating its potential use in rural clinics and point-of-care settings, where inexperienced clinicians may perform complex surgical procedures under real-time remote guidance of expert surgeons and physicians.

List of Abbreviations

SLN	sentinel lymph node
NIR	near infrared
ICG	indocyanine green
OR	operating room
LED	light-emitting diode
H&E	hematoxylin and eosin
RF	radio-frequency
MMP	matrix metalloproteinase

Acknowledgments

This study was supported in part by the US National Institutes of Health grants R01 EB008111 and EB 008458. Mr. Liu was supported in part by the US Department of Defense Breast Cancer Research Program Predoctoral Traineeship Award (W81XWH-11-1-0059). Dr. Akers was supported by Award Number K01RR026095 from the National Center for Research Resources. The content is solely the responsibility of the authors and does not necessarily represent the official views of the National Institutes of Health and the Department of Defense.

References

1. Collins L, et al. Outcome of Women with Ductal Carcinoma In Situ (DCIS) Treated with Breast-Conserving Surgery Alone: A Case-Control Study of 225 Patients from the Cancer Research Network. Modern Pathology. 2009; 22:34A–35A.
2. Vicini FA, et al. Impact of young age on outcome in patients with ductal carcinoma-in-situ treated with breast-conserving therapy. Journal of Clinical Oncology. 2000; 18:296–306. [PubMed: 10637243]
3. Albo D, et al. Anaphylactic reactions to isosulfan blue dye during sentinel lymph node biopsy for breast cancer. American Journal of Surgery. 2001; 182:393–398. [PubMed: 11720678]

4. Amr D, Broderick-Villa G, Haigh PI, Guenther JM, DiFronzo LA. Adverse drug reactions during lymphatic mapping and sentinel lymph node biopsy for solid neoplasms. American Surgeon. 2005; 71:720–724. [PubMed: 16468505]
5. Aydogan F, Celik V, Uras C, Salihoglu Z, Topuz U. A comparison of the adverse reactions associated with isosulfan blue versus methylene blue dye in sentinel lymph node biopsy for breast cancer. American Journal of Surgery. 2008; 195:277–278. [PubMed: 18194680]
6. Montgomery LL, et al. Isosulfan blue dye reactions during sentinel lymph node mapping for breast cancer. Anesthesia and Analgesia. 2002; 95:385–388. [PubMed: 12145056]
7. Thevarajah S, Huston TL, Simmons RM. A comparison of the adverse reactions associated with isosulfan blue versus methylene blue dye in for breast sentinel lymph node biopsy cancer. American Journal of Surgery. 2005; 189:236–239. [PubMed: 15720998]
8. Aarsvold JN, Alazraki NP. Update on detection of sentinel lymph nodes in patients with breast cancer. Seminars in Nuclear Medicine. 2005; 35:116–128. [PubMed: 15765374]
9. Wilke LG, et al. Rapid noninvasive optical imaging of tissue composition in breast tumor margins. American Journal of Surgery. 2009; 198:566–574. [PubMed: 19800470]
10. Troyan SL, et al. The FLARE((TM)) Intraoperative Near-Infrared Fluorescence Imaging System: A First-in-Human Clinical Trial in Breast Cancer Sentinel Lymph Node Mapping. Annals of Surgical Oncology. 2009; 16:2943–2952. [PubMed: 19582506]
11. Keller MD, Majumder SK, Mahadevan-Lansen A. Spatially offset Raman spectroscopy of layered soft tissues. Optics Letters. 2009; 34:926–928. [PubMed: 19340173]
12. Bydlon TM, et al. Rapid Optical Imaging of Breast Tumor Margins: Final Results from a 100-Patient Clinical Study. Cancer Research. 2009; 69:770S–771S.
13. Bhushan KR, et al. Detection of Breast Cancer Microcalcifications Using a Dual-modality SPECT/NIR Fluorescent Probe. Journal of the American Chemical Society. 2008; 130:17648. + [PubMed: 19055348]
14. Marzullo ACD, Neto OP, Bitar RA, Martinho HD, Martin AA. FT-Raman spectra of the border of infiltrating ductal carcinoma lesions. Photomedicine and Laser Surgery. 2007; 25:455–460. [PubMed: 17975961]
15. Zysk AM, Boppart SA. Computational methods for analysis of human breast tumor tissue in optical coherence tomography images. Journal of Biomedical Optics. 2006; 11 -
16. Haka AS, et al. In vivo margin assessment during partial mastectomy breast surgery using Raman spectroscopy. Cancer Research. 2006; 66:3317–3322. [PubMed: 16540686]
17. Lenkinski RE, Ahmed M, Zaheer A, Frangioni JV, Goldberg SN. Near-infrared fluorescence imaging of microcalcification in an animal model of breast cancer. Academic Radiology. 2003; 10:1159–1164. [PubMed: 14587634]
18. Zuzak KJ, Schaeberle MD, Gladwin MT, Cannon RO, Levin IW. Noninvasive determination of spatially resolved and time-resolved tissue perfusion in humans during nitric oxide inhibition and inhalation by use of a visible-reflectance hyperspectral imaging technique. Circulation. 2001; 104:2905–2910. [PubMed: 11739304]
19. Achilefu S, et al. Synthesis, in vitro receptor binding, and in vivo evaluation of fluorescein and carbocyanine peptide-based optical contrast agents. Journal of Medicinal Chemistry. 2002; 45:2003–2015. [PubMed: 11985468]
20. Yokoyama Y, et al. Value of indocyanine green clearance of the future liver remnant in predicting outcome after resection for biliary cancer. Br J Surg. 97:1260–1268. [PubMed: 20602507]
21. Liu Y, Solomon M, Achilefu S. Perspectives and potential applications of nanomedicine in breast and prostate cancer. Med Res Rev. DOI: 10.1002/med.20235.
22. Achilefu S, Dorshow RB, Bugaj JE, Rajagopalan R. Novel receptor-targeted fluorescent contrast agents for in vivo tumor imaging. Investigative Radiology. 2000; 35:479–485. [PubMed: 10946975]
23. Snoeks TJ, Khmelinskii A, Lelieveldt BP, Kaijzel EL, Lowik CW. Optical advances in skeletal imaging applied to bone metastases. Bone.
24. Bremer C, Tung CH, Weissleder R. In vivo molecular target assessment of matrix metalloproteinase inhibition. Nat Med. 2001; 7:743–748. [PubMed: 11385514]

25. Wang XH, Bhaumik S, Li Q, Staudinger VP, Yazdanfar S. Compact instrument for fluorescence image-guided surgery. Journal of Biomedical Optics. 2010; 15 -

26. Gotoh K, et al. HOW I DO IT A Novel Image-Guided Surgery of Hepatocellular Carcinoma by Indocyanine Green Fluorescence Imaging Navigation. Journal of Surgical Oncology. 2009; 100:75–79. [PubMed: 19301311]

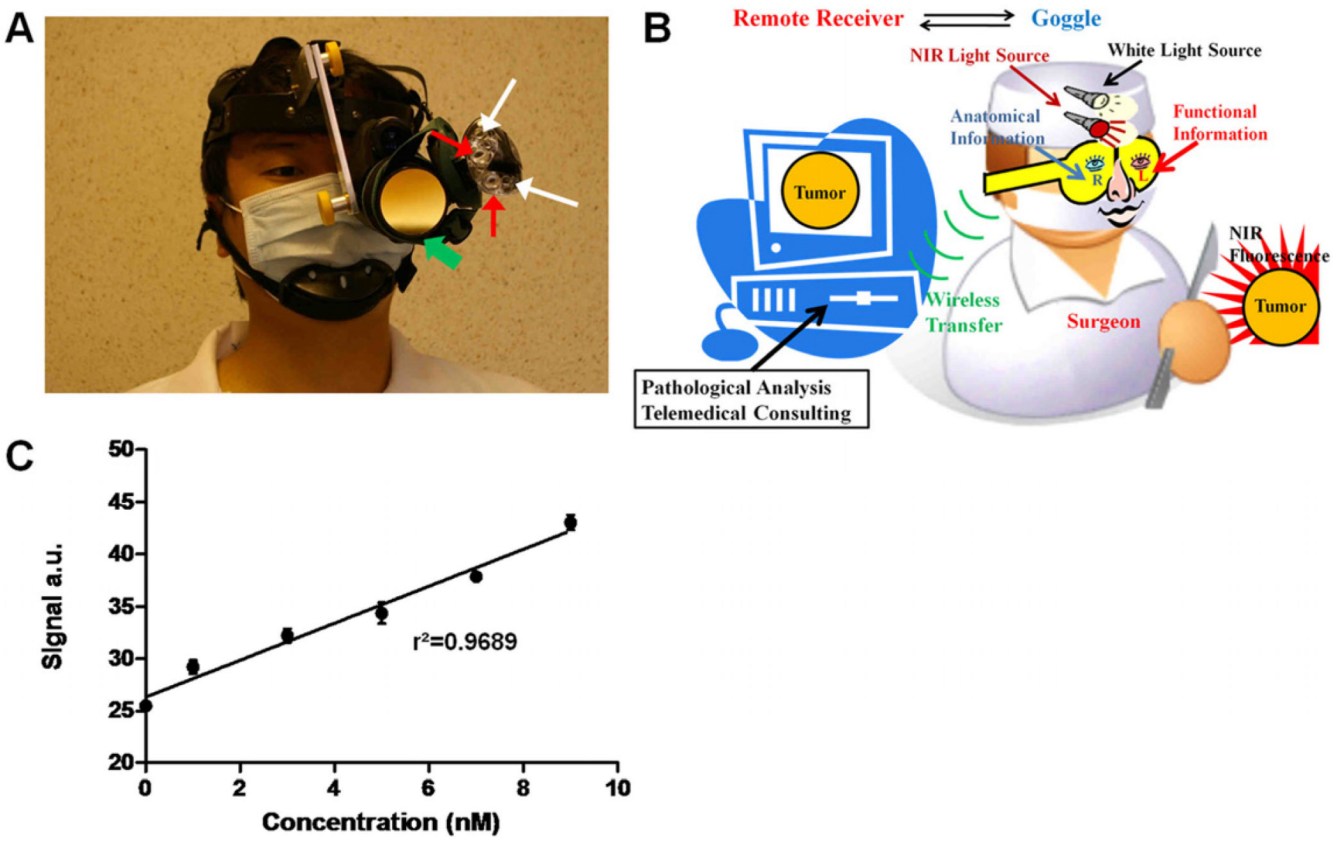

Figure 1.

Prototype intraoperative fluorescence imaging device. (**A**) Picture of the imaging device. Green arrows: detector; red arrows: NIR light sources; white arrows: white light sources. (**B**) Overview of the imaging system in a schematic diagram. Surgeon can capture functional information with one eye, while simultaneously obtaining anatomical information with the other eye. Real-time video can be transferred wirelessly to a remote site. (**C**) Sensitivity test of the device. NIR signal intensity versus indocyanine green concentration is plotted. Dots: mean values; error bars: standard deviation; r^2: linear regression coefficient.

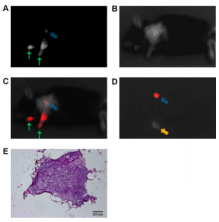

Figure 2.

NIR sentinel lymph node mapping with the imaging system and indocyanine green. (**A**) NIR fluorescence image of a mouse at 5 minutes post-injection. Blue arrow indicates the putative sentinel lymph node. Green arrows indicate the injection points. (**B**) White light image of a mouse at 5 minutes post-injection, acquired under room light illumination. (**C**) NIR-white light merge image mice at 5 minutes post-injection. NIR fluorescence is pseudo colored in red and superimposed on white light image. The blue arrow indicates the putative sentinel lymph node at an axilllary position. Green arrows indicate the injection points (**D**) *Ex vivo* inspection of resected lymph nodes shown in NIR-light merge image. NIR fluorescence is psedocolored in red and superimposed on white light image. A blue arrow indicates the putative sentinel lymph node removed from an axillary position, while a yellow arrow indicates an ischiatic lymph node taken from the hindquarter as non-fluorescent control. (**E**) Histology of resected SLNs showing a representative image of a frozen section of SLNs with H&E staining.

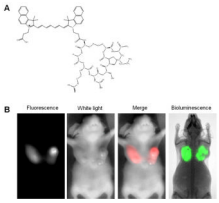

Figure 3.

NIR fluorescent probe LS 301 and tumor imaging (**A**) Structural illustration of LS 301. (**B**) Comparison of NIR fluorescence and bioluminescence images at 24 hours post-injection of LS 301. NIR fluorescence corresponds well with the bioluminscence in the tumor regions. NIR fluorescence and white-light images were acquired with the goggle device. Fluorescence was psedocolored in red in the fluorescence-white light merge image. Bioluminescence image and radiograph were captured with Carestream In-Vivo Multispectral FX PRO imaging system.

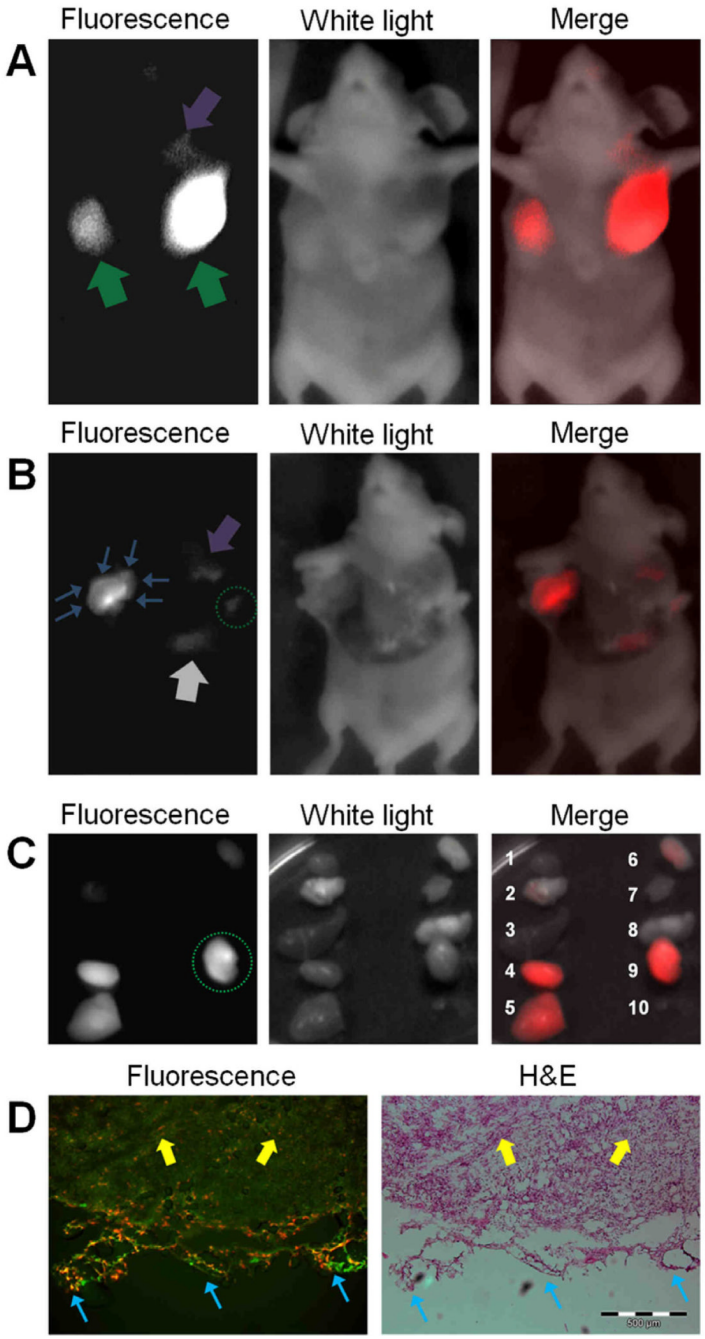

Figure 4.

Intraoperative tumor imaging with goggle device and LS 301. (**A**) Images of a mouse at 24 hours after intravenous injection of LS 301. NIR fluorescence (Left), White light (middle), and NIR-white light merge (right) images are shown. Major nodules in both breasts as well as small nodules can be clearly identified. Green arrows: major tumor nodules; Purple arrow: small tumor nodule. (**B**) Images of a mouse during tumor resection. Tumor margins emit high florescent signal, as shown in the bright “rim” of left tumor. Several residual tumors and small nodules that are non-obvious to naked-eye are also identified. Blue arrows: tumor margins at cross-section of a major nodule; Purple arrow: small tumor nodule; Grey arrow: liver; Green dotted circle: residual tumor intentionally left from previous resection.

(**C**) *Ex vivo* fluorescence, white light and merged images of tissues from dissected organs: 1.heart, 2.lung, 3.spleen, 4.kidney, 5.liver, 6.skin, 7. muscle, 8.brain, 9.tumor 10. blood. Resected tumor tissue shows high fluorescent signal (Green dotted circle). Liver and kidney also exhibit high fluorescence level as they are the major organs responsible for excretion and metabolism of imaging agents. (**D**) Fluorescence and color microscopy of resected tumor tissues. Merged autofluorescence (480ex/535em, green) and LS301 NIR fluorescence (775ex/810em, red) (left) along with color microscopy after H&E staining of the same section (right). High NIR florescence from LS 301 was found in the tumor, as well as on the margin, as shown in red color on the left image. Yellow arrows: tumor proper; Blue arrows: tumor margin.

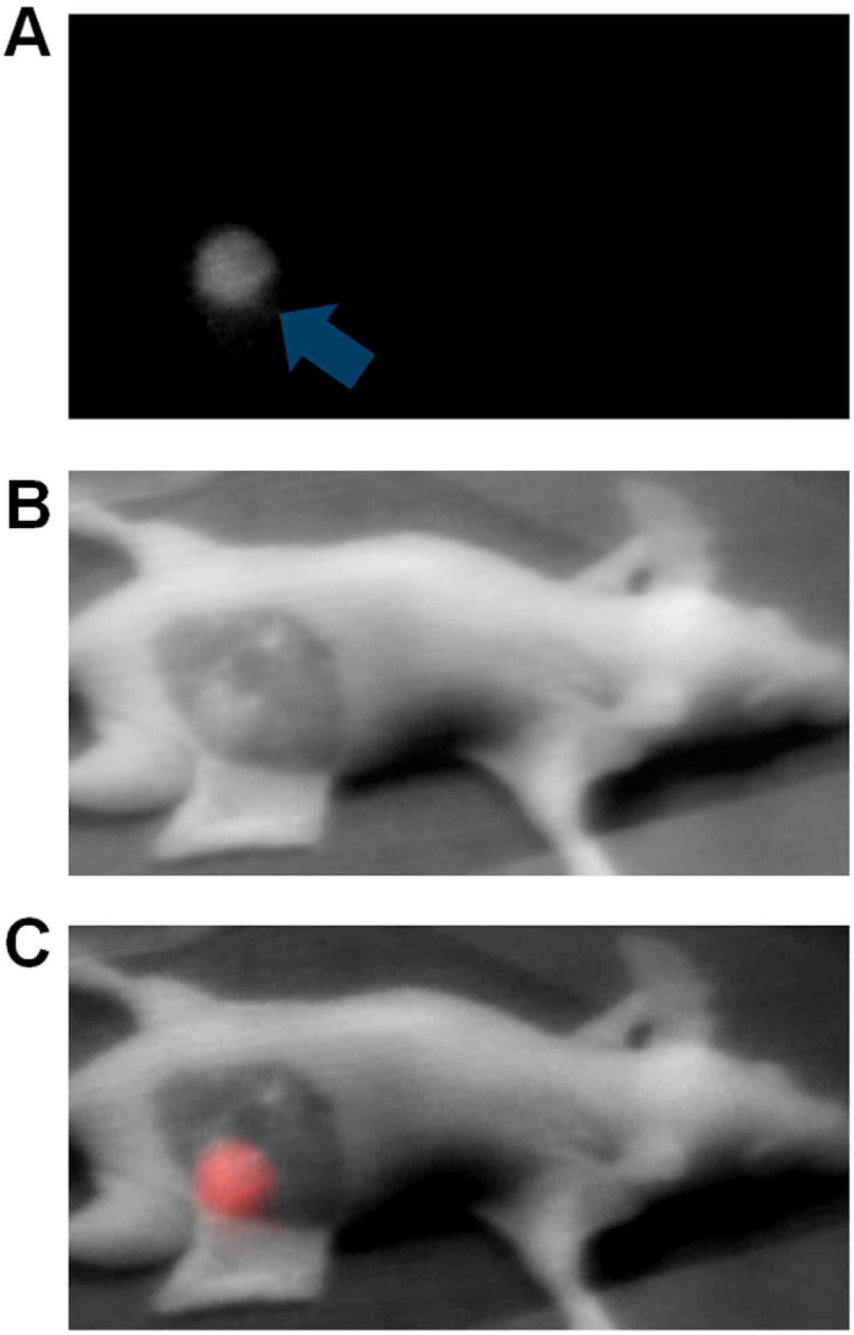

Figure 5.
Fluorescence-guided surgery images acquired via wireless transfer. Real-time video was transferred to remote computer using a RF transmitter/receiver set. (**A**) NIR fluorescence image, (**B**) white light, and (**C**) merged image of mouse 24 hours post-injection demonstrating the high signal from tumor tissue prior to resection.